Stratigraphic reconstruction of the Ediacaran Yangtze Platform margin (Hunan Province, China) using a large olistolith

E. Vernhet [a],*, C. Heubeck [a], M.-Y. Zhu [b], J.-M. Zhang [b]

[a] *Institut für Geologische Wissenschaften, Freie Universität Berlin, Malteserstrasse 74-100, D-12249 Berlin, Germany*
[b] *Nanjing Institute of Geology and Palaeontology, 39 Beijing Donglu, Nanjing 210008, Jiangsu Prov., P.R. China*

Abstract

The southeast-facing slope of the Yangtze platform during deposition of the Ediacaran Doushantuo Formation included several submarine slides and olistostromes of regional extent. These platform margin-derived slides provide windows into the contemporaneous platform margin. This manuscript proposes a paleoenvironmental reconstruction and evolution of the Ediacaran Yangtze platform margin using facies analysis of one of these large-scale slide sheets, which transported shallow-marine platform facies. The base of the slide sheet shows dolomite, chert, evaporites, and phosphorites, lithological association with "tepee" structures and storm-induced microbreccia. Dolomitised limestones with current-related sedimentary structures overlie these facies. Thus, the Ediacaran Yangtze platform may have evolved from a shallow, rimmed platform with shallow, restricted, back-rim, basins developed on the margin to a wave-dominated, shallow subtidal platform. Sequence analysis applied to the slide sheet sediments allows relative dating of the sliding.

1. Introduction

The Ediacaran and Cambrian strata of the Yangtze platform are one of the foremost locations worldwide to study the conditions and setting of the Cambrian bio-radiation. A detailed understanding of the temporal sequence and ecologic drivers of this radiation event has been hindered both by a lack of detailed correlation between the numerous important fossil-bearing locations (e.g., Miaohe biota, Hubei Province (Xiao et al., 2002); Weng'an biota, Guizhou Province (Yin et al., 2001, 2004; Chen et al., 2004), Chengjiang biota, Yunnan province (Chen et al., 1991, 1999; Babcock and Zhang, 2001; Babcock et al., 2001; Hou and Bergstrom, 2003; Hou et al., 2004; Shu et al., 2004), and by a poor understanding of the acting sedimentology processes. In the transition zone between the fossiliferous, shallow-marine, stratigraphically incomplete carbonate environment and the deep-water, stratigraphically complete but mostly fossil-free siliciclastic environment, may lie the potential to reconstruct a detailed stratigraphic framework for the Ediacaran Yangtze platform.

This study focuses on the southern margin of the Yangtze platform in Hunan province where the Ediacaran slope is well exposed. Four margin-derived slide sheets in the Doushantuo Formation slope have been

* Corresponding author. Actual address: Département des Géosciences, Université de Franche-Comté 16, route de Gray, 25000 Besançon, France.
E-mail address: vernhet.elodie@voila.fr (E. Vernhet).

identified. This manuscript gives a paleoenvironmental reconstruction of the Yangtze platform margin using detailed facies analysis of slide sheet sediments and proposes a correlation between the platform margin-derived slide and a platform type section.

2. Location and geological setting

All studied sections are located in Hunan province (Fig. 1), set in the south-facing slope environment (Steiner, 2001; Vernhet, 2007) of the Ediacaran Yangtze platform (Fig. 2). Two sections (Wuhe and Xikou) in Guizhou province complete these data. At present, the Yangtze platform is bounded to the north by the Qin-Lin fault, extending from Tibet to northern Anhui, and to the southeast by the Cathaysia suture. Its current setting is the result of Yangtze microplate collision with the Cathaysia arc to the SE during the Silurian and with the North China craton to the north during the early Triassic (Kenneth and Chen, 1999). These collisions deformed the Paleozoic sedimentary cover of the Yangtze platform only moderately. Cretaceous extension created large, fault-bounded basins filled by continental-facies lithologies. Generally, Proterozoic–Paleozoic strata are preserved in a thickness of several kilometres and have been moderately folded on a large scale. The location of the South China craton during the Ediacaran, and its place in the Rodinia supercontinent, like that of many other small cratons, is poorly known. Paleomagnetic analyses indicate an
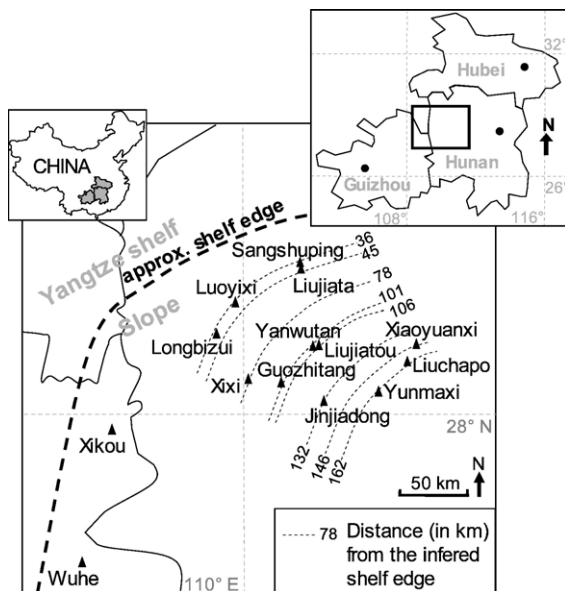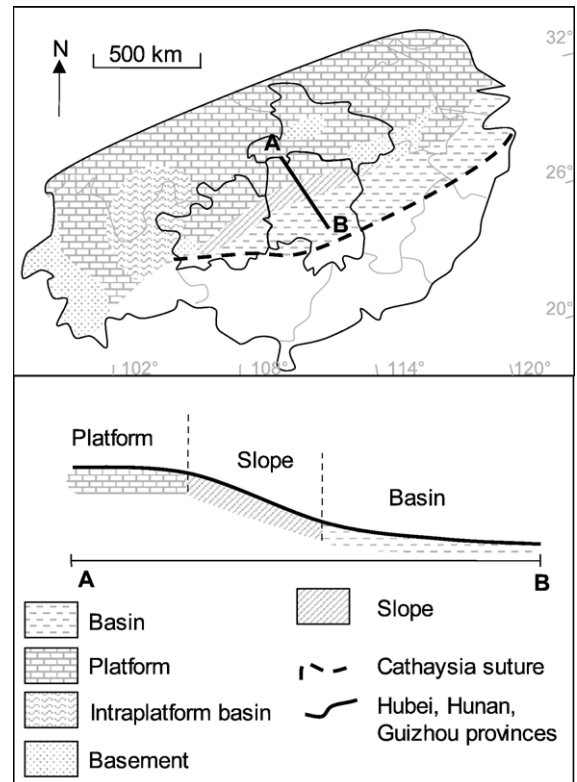

Fig. 2. Paleoenvironmental reconstruction of the southern Yangtze craton during the late Ediacaran (Doushantuo Fm; ~635–550 Ma (Condon et al., 2005)) (in part modified after Steiner, 2001).

equatorial position (Macouin et al., 2004) at 600 Ma. Li et al. (1995) proposed that the South China plate linked Australia with Laurentia from 1 Ga to 700 Ma. Powell and Pisarevsky (2002), in their reconstruction of Gondwana and Laurentia, also join South China with Australia. According to Condie (2003) and Pisarevsky et al. (2003), the Yangtze platform and Cathaysia (southeastern part of present-day China) collided to form the South China craton already during the Meso- and early Neoproterozoic, before they separated again during Rodinia breakup. Since then, the general tectonic setting was extensional, and the platform evolved as a passive margin after the Ediacaran (Wang and Li, 2003).

3. Stratigraphic succession

Formation names change regionally mostly due to lithological and facies changes. Erdtmann and Steiner (2001), Wang and Li (2003), and Zhu et al. (2004) propose a correlation frame for the Yangtze platform from the Ediacaran to the Cambrian. The Ediacaran stratigraphic succession in Hunan province (Fig. 3) begins with the thick diamictites of the Nantuo Formation. The glacial

Fig. 1. The study area (largely in northern Hunan Province in central China) representing the Ediacaran south-facing slope of the Yangtze craton.

Age (Ma)	Syst.	Hunan Formation names
— 530	CAMBRIAN	Xiaoyanxi Fm
— 542		Liuchapo Fm
— 551 (1)	EDIACARAN	Doushantuo Fm
— 635 (1)	CRYOGENIAN	Nantuo Fm

Fig. 3. Schematic stratigraphic column for the Ediacaran and basal Cambrian of south-central China ((1) Condon et al., 2005).

character of the Nantuo Formation is locally doubtful (Bahlburg, 2004; Dobrzinski et al., 2004; Eyles and Januszczak, 2004; Dobrzinski and Bahlburg, 2007-this volume). Its age is also debated: Evans et al. (2000), and Wang and Li (2003) argue for a "Sturtian" age (approximately 750 Ma, Frimmel et al., 2002), whereas Jiang et al. (2003), Chen et al. (2004), and Zhou et al. (2004) propose that Nantuo tillites are time-equivalent to the Marinoan glaciation (approximately 663 Ma, Knoll and Xiao, 1999; approximately 635 Ma, Condon et al., 2005). The thickness of the Nantuo Formation ranges from 0 to more than 2000 m, its maximum reported in the northern Guangxi province (Wang and Li, 2003). Wang and Li (2003) argue that the Nantuo Formation represents the latest stage of the rifting during Rodinia breakup. These partially glaciogenic sediments attracted renewed interest with the "Snowball Earth" hypothesis (Hoffman et al., 1998; Hoffman and Schrag, 2000; Hyde et al., 2000; Runnegar, 2000; Hoffman and Schrag, 2002). A "cap carbonate" of approximately 6 m thickness overlies the diamictites and forms the basal unit of the Doushantuo Formation. U–Pb dating on zircons yields an age of approx. 635.2 ± 0.6 Ma (Condon et al., 2005). These carbonates show unusual sedimentary structures (Sumner, 2002; Nogueira et al., 2003) and a negative $\delta^{13}C$ isotope anomaly (Knoll et al., 1993; Germs, 1995; Corsetti and Hagadorn, 2000), marking a sudden Ediacaran change from icehouse to greenhouse conditions. The Nantuo Formation "tillites" and the Doushantuo Formation "cap carbonate" extend regionally throughout the central and southern Yangtze Platform.

The remainder of the Doushantuo Formation in Hunan province, a deep-water environment below wave base, is dominated by black, thinly laminated, silicified shales, interbedded with thinly bedded, dark-grey siltstones representing turbidity current deposits, rare, thinly laminated cherts, and two, regionally traceable phosphorite horizons which are also present on the platform (Zhu et al., 2004). Allochthonous dolomitized limestone intervals with current-induced sedimentary structures, gently deformed by soft-sedimentary deformation, locally interrupt the autochthonous black shales. These limestone intervals, reaching up to 60 m in stratigraphic thickness, are surrounded by slope facies sediments, and can be correlated using their stratigraphic position, lithology, and facies over large distances (>50 km). These allochthonous limestone intervals are considered as mega-olistoliths or slide sheets (Vernhet, 2005; Vernhet et al., 2006). The carbon isotopic evolution shows a shift in the $\delta^{13}C_{org}$ value, which may highlight also the presence of slide sheets (Guo et al., 2007-this volume). Tuffaceous beds are common, but thin, and commonly discontinuous. Most shales contain minor or variable tuffaceous components.

The contact between the Doushantuo Formation and the overlying Liuchapo Formation is drawn at the first occurrence of thick-bedded silicified shales. This contact is commonly erosive. In several sections, it represents the base of a thick allochthonous sequence involving olistostromes and large-scale contorted bedding. The silicified black shales of Liuchapo Formation grade updip into dolomitized limestone of the approximately time-equivalent Dengying Formation, which is widespread in the Yangtze platform-facies of northern Hunan and Hubei Provinces (Fig. 3).

4. Data

4.1. Olistostrome facies description and interpretation

Four major slide events are regionally traceable in the slope sections of Hunan province (Fig. 4). In slide sheets, the internal sedimentary sequence is preserved and therefore allows reconstruction of the paleoenvironment of the platform margin and its evolution over time. The following facies analysis is focused on the largest and thickest of the four mass-flow events, slide sheet no. 3 (Fig. 4), which occurs in almost all studied sections and shows a broad facies diversity. The facies analysis was supported by approximately 20 hand samples and 30 thin sections. Additional observations at outcrop scale contribute to our conclusions. Diagenesis masks a large part of the initial lithology. The phosphorites do not show any late diagenetic replacement features; however,
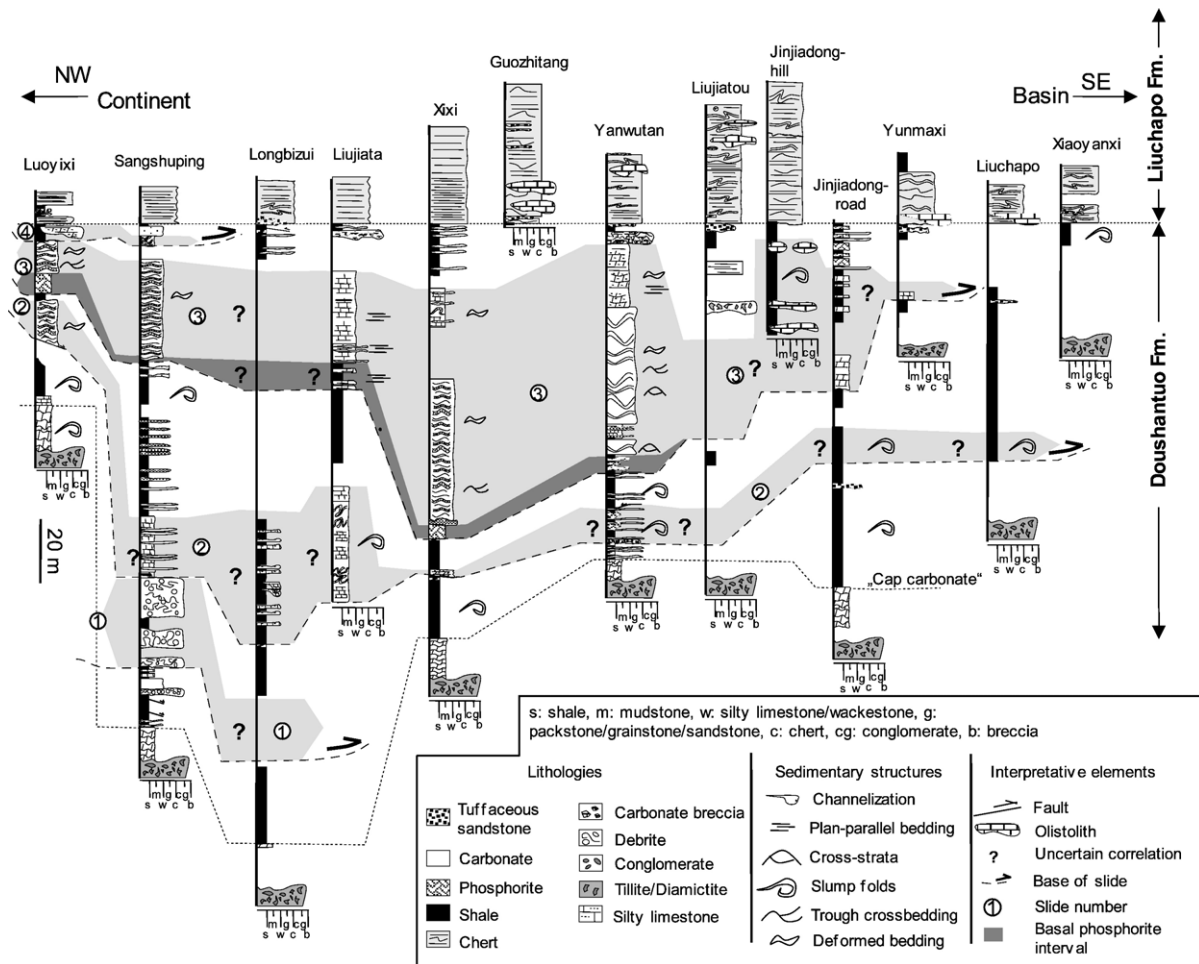
Fig. 4. Stratigraphic correlation diagram between key sections in the Hunan province (slides 1 through 4) on the south-facing slope of the Yangtze platform. See Fig. 1 for the location.

evaporites are nearly all replaced by calcite or quartz and identifiable as pseudomorphs only. In the slide sheet, as in the autochthonous slope sediments, the bedding is gently folded by secondary deformation due to gravity-related processes. Lithologies and sedimentary structures of slide sheet no. 3 sediments can be grouped and assigned to three facies distributed in two facies associations.

4.1.1. Micrite-dominated facies association

4.1.1.1. Facies 1

4.1.1.1.1. Description. Thinly laminated, pink dolomites are interbedded with patchy, black, thinly laminated silicified mudstones. Few cm-scale "tepee structures" deform locally the silicified mudstones and are onlapped by cherty beds (Fig. 5A). Internal erosion surfaces are marked by black laminae (Fig. 5B). At the outcrop scale, this interval measures approximately 2 m

in thickness. The contact with the underlying, deformed, autochthonous black shales is erosive. The contact with the overlying, allochthonous, silty laminated limestones is sharp and parallel. In thin section, the samples show millimetre-sized radially organised quartz crystals (Fig. 7A). Light beige carbonate or phosphatic micrite is interbedded with dark bituminous laminations. Patchy apatite cement is rare. This facies is particularly well represented in Luoyixi section. In Yanwutan section, very thin-bedded, very fine-grained dolomitized grain-stones/packstones are interbedded with silicified evap-orite-bearing dolomite and phosphorite.

4.1.1.1.2. Interpretation and depositional environment. Dark bituminous laminations are interpreted as biomats preserved by early diagenetic silica cementation of mudstone. Hypoxic conditions under the biomats may have allowed the concentration of fluoroapatite and the subsequent precipitation of rare early-diagenetic
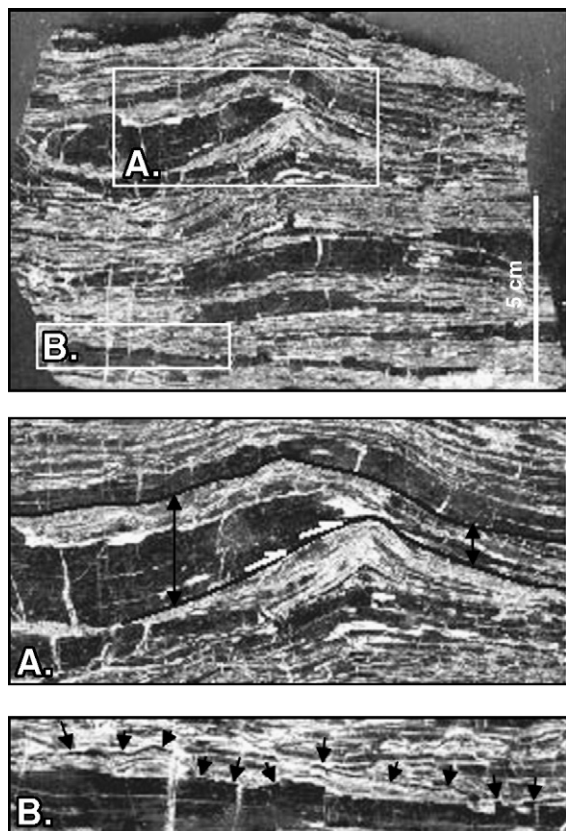
Fig. 5. Facies 1 showing evidence for occasional emergence in Luoyixi section (Hunan province): (A) Small-scale thickness variations marking sediment onlap on "tepee structure". (B) Small-scale internal erosion surface marked by possible biomats. Dimensions of the hand sample are 8 cm*12 cm.

patchy phosmicrite. The small-scale onlaps indicate that the "tepees" are likely the result of early diagenetic sediment dewatering during exposure to the atmosphere rather than dewatering during burial. Thus, in Luoyixi section, the sedimentation is entirely dominated by suspension settling and (bio-) precipitation. In Yanwutan section, the presence of fine-sand-grained dolomitized grainstones/packstones in the allochthonous block indicates that the original location of the displaced block may have been subjected to medium-energy events. The micrite-dominated facies association suggests a low-energy, protected environment, shallow enough to be temporarily emergent and to allow the formation of "tepee" structures by subaerial dewatering of sediments. A rim or sand shoal may have acted as a barrier between the protected back-rim basins and the open ocean. In Yanwutan, fine-grained grainstones indicate that locally the rim may have been submerged by open ocean waves.

4.1.1.2. Facies 2

4.1.1.2.1. Description. Facies 2 is characterised by two types of phosmicrite, interbedded with evaporite-bearing dolomicrite (Fig. 6A, B, C). The phosmicrites have been subjected to reworking resulting in dolomicrite-supported microbreccia with millimetre-sized phosintraclasts (Fig. 6F) and highly deformed dolomicrite-supported breccia with cm-sized phosintraclasts (Fig. 6G). At the outcrop scale, this phosphoritic interval is approximately 1.5-to-2-m-thick. The phosmicrites can be grouped as either "soft" phosphorite or "hard" phosphorite, depending on their response to applied stress. "Soft" phosphorites show 1-to-5-cm-thick beds of reddish-brown, thinly laminated phosmicrite (Fig. 6B, C). Locally, in breccia facies, these phosphorites are closely mixed with dolomite beds. Thin section examination demonstrates that laminations consist of approximately 200 µm-thick couplets of basal organic matter-rich, black beds overlain by thin phosmicrite. Apatite and calcite-filled spheres, possibly microfossil remnants, interrupt the laminations (Fig. 6D, E).

The "hard" phosphorites consist of centimetre-thick, dark brown to black phosmicrite beds (Fig. 6A, B, C), including millimetre-sized, calcite-filled, round, unidentified fossils. Small pyrite crystals are common. These phosmicrites show a brittle behaviour and are the main source of clasts during reworking in microbreccia and breccia. In thin section, structureless opaque-brownish micrite is interbedded with thin organic-matter-rich, opaque laminations. The bases of the beds have a sharp, regular conformable contact with underlying dolomite or "soft" phosphorite. In contrast, their tops may be erosional.

Micro-breccias (Fig. 6F) show 2-to-5-cm-thick beds with approximately 0.5-cm-sized "hard" phosphorite intraclasts in a dolomite matrix. The dolomite matrix shows an irregular, complex network of curved, calcite-filled fractures. Contacts between the microbreccia and underlying phosmicrite are erosive. In thin sections, fractures in the dolomicrite matrix appear to be part of millimetre-sized collapse breccias and small-scale enterotrophic structures (Fig. 7E). Phosmicrite constitutes the intraclasts.

Dolomicrite-supported breccias (Fig. 6G) include cm-sized "hard" phosphorite intraclasts which may be aligned and form decimetre-sized tight folds. The dolomite matrix is veined by an irregular, complex network of small-scale (millimetre-sized), curved fractures filled by calcite, which gives to the lithology a highly deformed appearance. In the 15 samples examined, the "hard" phosphorites show variable degrees of deformation, ranging from thin fractures to complete disorganisation of beds (Fig. 12). In thin section,
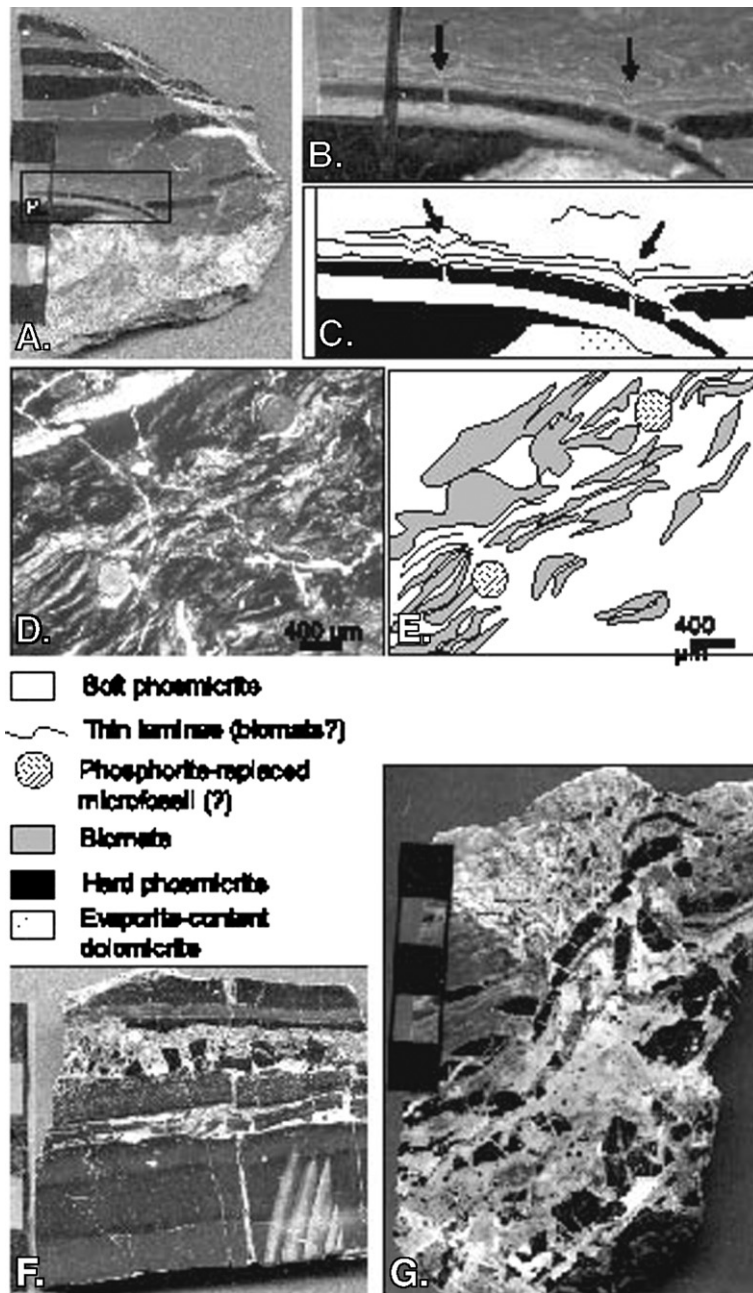
Fig. 6. Facies 2, samples from the Xixi section, Hunan Province. (A, B and C) Hand samples and interpreted line drawings showing internal structures of soft phosmicrites. Biolaminations deform plastically (black arrows) while black, hard phosmicrites deform brittley. (D and E) Thin section photomicrograph (D) and line drawing of "soft phosmicrite". Spherical microfossils (?) interrupt biolaminations. (F) Microbreccia with half-cm-sized clasts of phosphorite hardground ("hard phosmicrite"), scale bar is 5 cm long. (G) Tight fold defined by centimetre-sized phosphorite-clast breccia hardground ("hard phosmicrite") due to precipitation and dissolution of evaporites in a dolomicrite matrix, scale bar is 5 cm long.

palisade calcite commonly surrounds phosphorite clasts. Acicular (Fig. 7B, F) and lozenge-shaped calcite crystals and fan-shaped calcite crystals (Fig. 7C, D) are common. 0.5-to-1-cm-thick, "contoured" calcite veins without preferential orientation, and centimetre-thick collapse breccias are abundant (Fig. 7E).

4.1.1.2.2. Interpretation and depositional environment. Phosmicrite precipitation requires a low-energy environment with low sedimentation rates and semi-anoxic conditions (Liang and Chang, 1984; Yiqing, 1984; Föllmi et al., 1991; Trappe, 1998, 2001). These allow, on one hand, the accumulation of organic matter (Baturin,
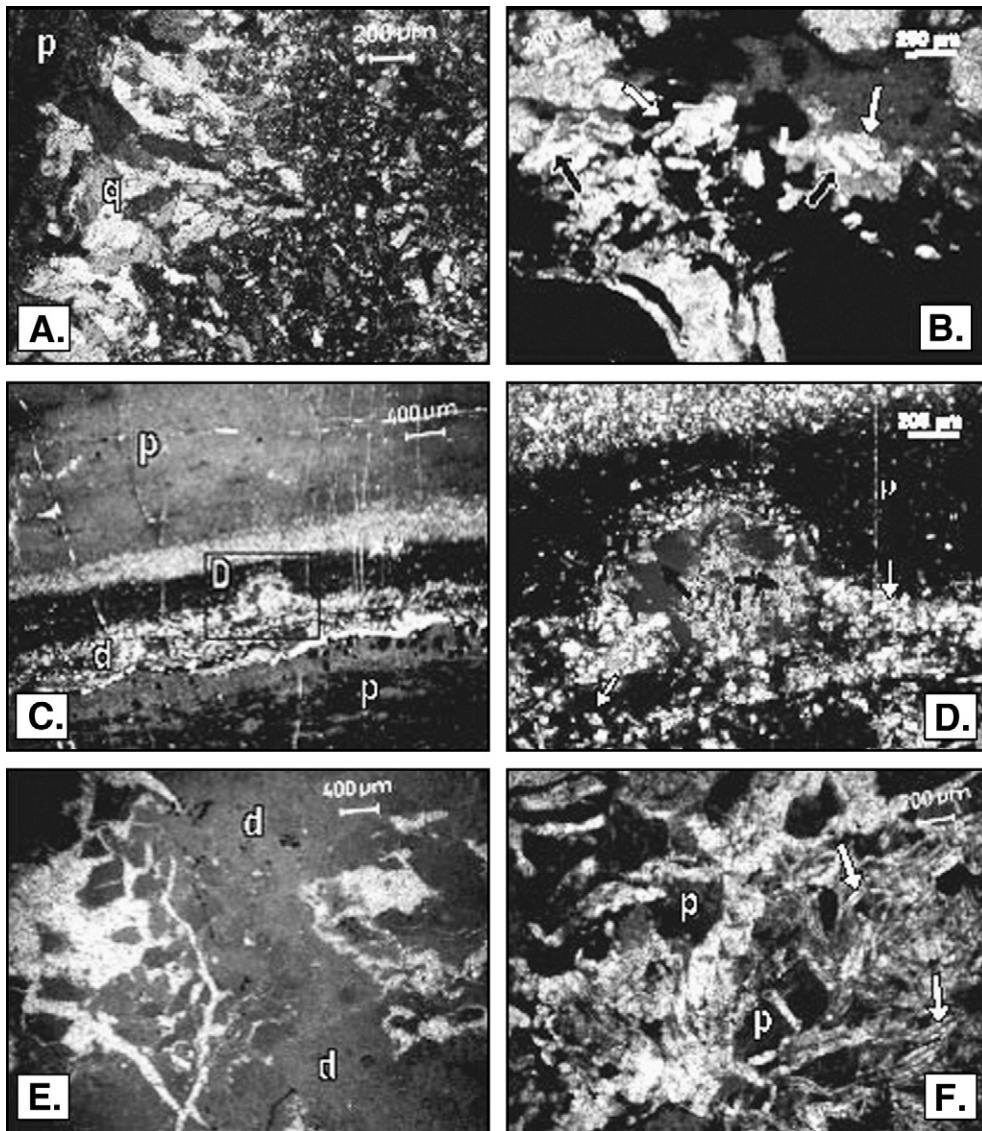
Fig. 7. Evaporites and their pseudomorphs in thin section from olistoliths in Xixi section (except D: Luoyixi section). p: phosphorite, d: evaporite-content dolomite, q: quartz. (A) Large quartz crystals replacing gypsum (Facies 1). (B) Anhydrite pseudomorphs after gypsum (white arrows) and calcite pseudomorphs after gypsum (black arrows) in (evaporite-content) dolomicrite-supported breccia (Facies 2). (C) Microdome of fan-shaped gypsum pseudomorphs (Facies 2). (D) Detail of A. Note radial growth of calcite replacing gypsum (black arrows) and the well developed, euhedral dolomite crystals (white arrows; Facies 2). (E) Evaporite-bearing dolomicrite with (to the right) small-scale, calcite-filled fractures organised in enterotrophic (coalescent small-scale nodules) structures and small-scale collapse breccia (left) due to local dissolution of evaporites (Facies 2B). (F) Calcite cement replacing anhydrite. Note the acicular crystals between phosphorite intraclasts (Facies 2B).

1982) and, on the other hand, partial degradation of organic matter, allowing phosphate to saturate the pore water (Trappe, 1998; Schwennicke et al., 2000). In this study, phosphorites are associated with biomats (organic matter-rich beds) and mudstones, which may have acted as impermeable barriers and prevented fluid exchange with oxygenated water (Schwennicke et al., 2000). Microbial activity favours phosphogenesis by degradation of organic matter (Föllmi et al., 1991; Trappe, 1998),

thereby providing a proximal source of phosphorus. Phosphorite sedimentation requires a low-energy environment in which the water column remains stratified, causing precipitation of apatite in the uppermost 10 cm of sediments (Föllmi et al., 1991). The organisation of the phosmicrites in hand samples appears to alternate between periods of elevated sediment supply (which may have induced the sedimentation of "soft" phosphorite beds) and periods of sediment "starvation", which allow

formation and erosion of "hardgrounds" represented by the "hard" phosphorite beds. "Hard" and "soft" phosphorites are reworked to micro-breccias and breccias.

Microbreccias represent short-distance transport of phosmicrite hardground chips, eroded from underlying beds, and reworked by currents. These microbreccias may record occasional medium-to high-energy events such as storms.

The formation of breccia with centimetre-sized clasts as observed in hand samples may be related to primary or early diagenetic evaporite growth and dissolution (Fig. 12). As a result, competent phosmicrite beds have

fractured to accommodate the deformation. Semi-consolidated dolomicrite mud flowed into these fractures and facilitated subsequent deformation (Fig. 6A, B, C). Evidence of evaporite presence in hand samples indicates that palisade calcite and the acicular, lozenge- and fan-shaped calcite crystals (Fig. 7B, C, D, F) observed in thin section may possibly represent replaced palisade gypsum and pseudomorphs after anhydrite, respectively.

Therefore, the phosmicrites in the study area were likely deposited in a restricted basin with high organic matter content and semi-anoxic conditions. The episodic
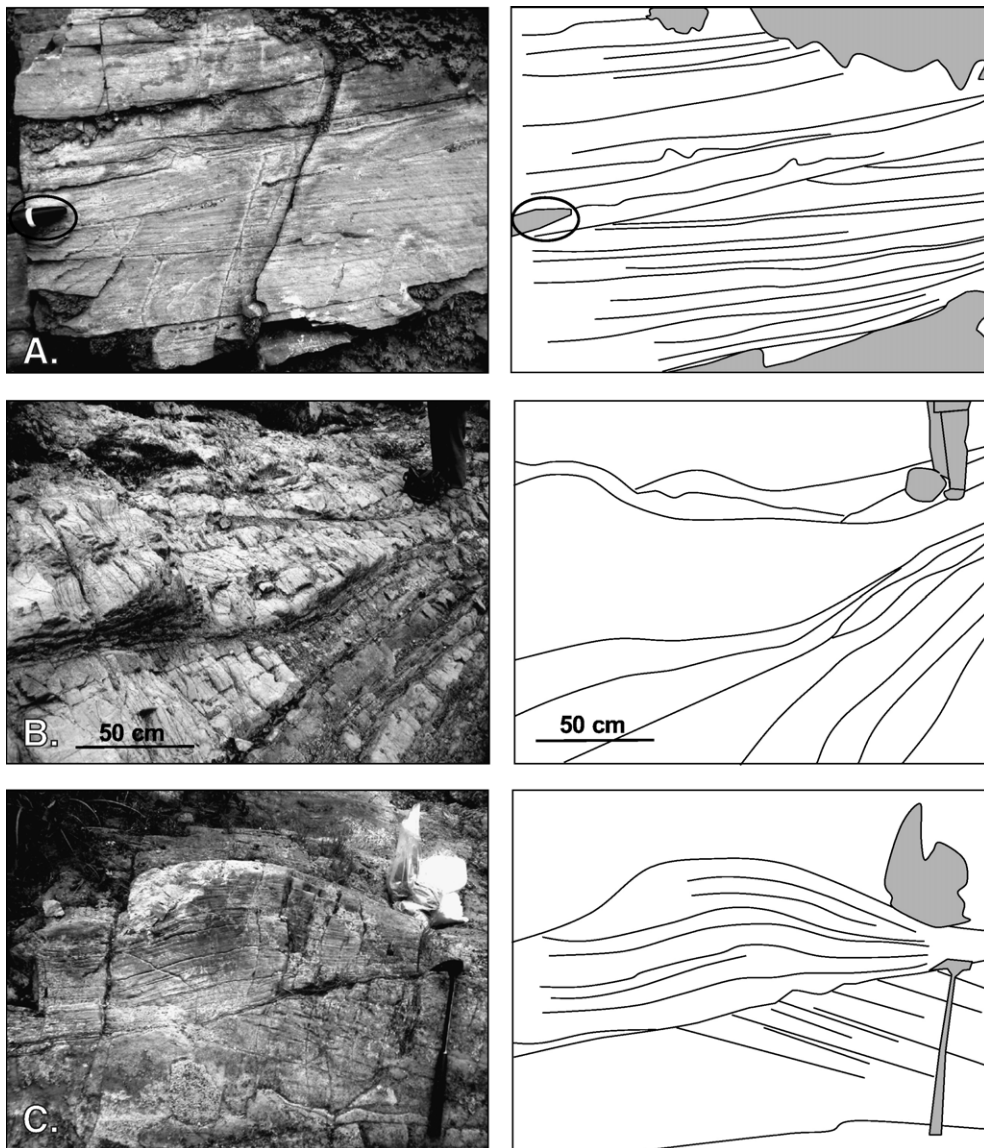

Fig. 8. Outcrop view of Facies 3. (A) Silty dolomitized limestones with trough cross-bedding deposited above the fairweather wave base. Pen tip ~2 cm long; Luoyixi section. (B) Large-scale cross-strata with internal cross-bedding representing sand shoals. Scale is 50 cm long; Yanwutan section. (C) Cross-bedding formed by mega-ripples. Geological hammer for scale is 40 cm long; Yanwutan section.

deposition of thin evaporite-content dolomicrite beds indicates temporary evaporative conditions and suggests rhythmic variations of the sedimentation rate in the succession of phoscrete hardgrounds ("hard" phosphorite), evaporite-bearing dolomitized limestones, and clay-rich phosmicrites ("soft" phosphorite) colonized by biomats. The evaporitic conditions argue for a shallow-water, protected depositional environment.

4.1.2. Grainstone-dominated facies association

4.1.2.1. Facies 3. Facies 3 usually overlies Facies 1 and 2 of the micrite-dominated facies association. At the outcrop scale, this interval ranges from approximately 5-to 30-m-thick and consists of silty limestones, grainstones, or packstones with current-induced sedimentary structures. These facies are subdivided into
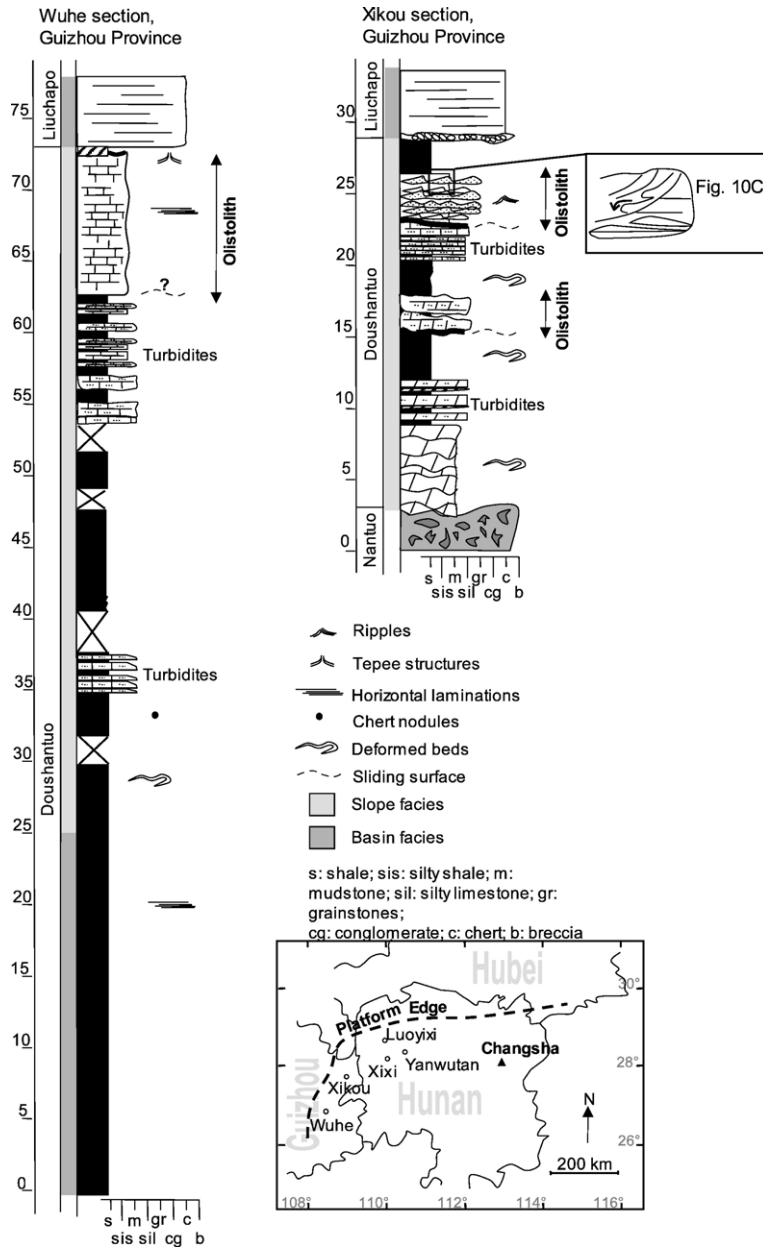

Fig. 9. Stratigraphic columns of the Wuhe and Xikou sections in Guizhou province documenting the presence of olistoliths with shallow-water platform facies in the slope facies.

three facies according to their preserved sedimentary structures at the outcrop scale.

4.1.2.2. Facies 3A. This facies shows 3-to-10-cm-thick, horizontally laminated packstones (e.g. Xixi section) or silty dolomitized limestones with cm-sized trough cross-bedding (e.g. Luoyixi section) (Fig. 8A). On the outcrop, this facies comprises 10-to-30-m-thick intervals without lithology or sedimentary structure changes.

4.1.2.3. Facies 3B. This facies includes 0.5-to-1-m-thick cross-stratified dolomitised grainstones/packstones (Fig. 8B) (e.g., Yanwutan section). No grain-size gradation has been observed. In thin section, this facies shows secondary euhedral dolomite rhombs with some pyrite crystals, rendering the identification of the primary microfabric impossible.

4.1.2.4. Facies 3C. This facies consists of medium-sand-grained, cross-stratified dolomite with trough, decimetre-sized cross-bedding (Fig. 8C). In thin sections, euhedral, well-developed crystals of secondary dolomite mask the primary lithology of this interval; however, the sedimentary structures argue for a grainstone facies (e.g. Yanwutan section).

4.1.2.4.1. Interpretation and depositional environment. The scale of observed sedimentary structures, the absence of grain size gradation, and the absence of other decreasing current evidence exclude the interpretation of Facies 3 as turbidite deposits. The 10-to-30-m-thick intervals of Facies 3A may indicate that the current, which allows the formation of ripples (expressed by trough cross-bedding in vertical profile) or low-energy horizontal bedding, was permanent. The Facies 3A may have been deposited in an almost permanently wave-agitated environment. Facies 3B and 3C show stratifications, possibly hummocky cross-stratifications and sand mega-ripples, which may have been formed by storm events or platform currents. This facies association indicates a depositional environment above the storm wave limit (commonly 100 m). The predominance of trough cross-bedding suggests a water depth near the fair-weather wave base (commonly 30 m).

Thus, Facies 3 shows characteristic facies associations of a wave- and storm-dominated, shallow-water subtidal platform. The medium- to high-energy, open-marine, cross-stratified Facies 3 overlies the phosphoritic facies and indicates that the rim that protected back-rim shallow-water restricted basins has been removed, allowing coastal currents to rework the platform sediments and to allow grainstone sedimentation.

4.2. Platform margin drowning structures in Guizhou province

Other olistromal deposits appear to occur for several 100 km westward into Guizhou Province (Fig. 9). An approximately 10-m-thick olistolith in Wuhe section, Guizhou Province, is located near the top of the Doushantuo Formation. The block consists of brown-beige, cm-thick, interbedded dolomitized mudstones/wackestones/packstones, with desiccation crack structures forming polygons on bedding surfaces. A 3-cm-thick bentonite overlies the carbonate blocks and separates it from autochthonous cherts and silicified shales of the overlying Liuchapo Formation. The approximately 60-m-thick underlying autochthonous section consists predominantly of shales. Its depositional environment is difficult to determine due to the absence of identifiable sedimentary structures. However, deformed beds approximately 30 m above section base and the presence of an olistolith argue for a slope environment, possibly underlain by basin facies. The base of the section is poorly exposed (Fig. 9).

The base of Xikou section, Guizhou Province, exposes Nantuo Formation diamictites and a 5-m-thick "cap dolomite" with slump structures, overlain by 20-m-thick shales and turbidites. Two olistoliths interrupt the suspension and turbiditic sedimentation. The lower block at approximately 15 m from the base of the section shows silty limestones (Fig. 10A). Its shallow-water character is not evident. The second olistolith, above an erosive contact with the underlying turbidite deposits (Fig. 10B), occurs 10 m higher and shows fine-grained grainstones to packstones and wackestones with common sigmoidal ripples (Fig. 10C) draped by thinly laminated wackestones (Fig. 10D) that most closely resemble structures formed in intertidal environments. Intraformational channels cut and erode the set of ripples. Purple shales with microbial structures followed by Liuchapo Formation chert overlie the sliding block. We interpret the entire section of the Doushantuo Formation in Xikou section as a submarine slope, affected by mass wasting.

5. Discussion

5.1. Relative dating of slides

The slope sedimentation process involving displacement of large slide sheets limited their internal deformation and largely conserved the original stratigraphy of these platform margin deposits (Vernhet, 2005). Therefore, a correlation of allochthonous olistostrome-internal
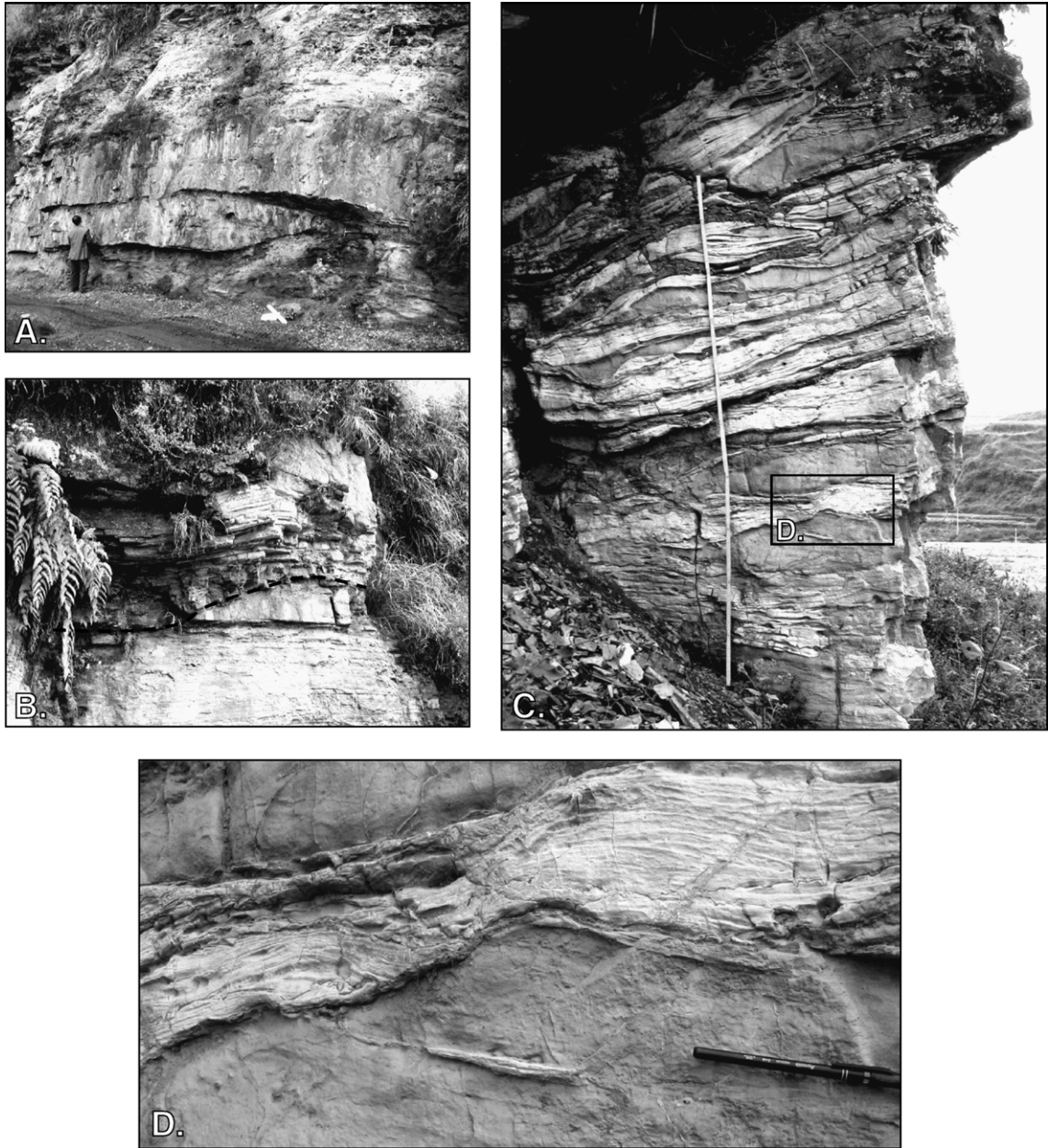
Fig. 10. Outcrop photographs of olistoliths at Xikou section, Guizhou province. (A) Lower olistolith involving silty limestones. Note the lenticular shape and the highly deformed surrounding black shales. (B) Erosive base of the upper olistolith. The shelf-edge-derived block is in erosional contact with autochthonous slope sediments. (C) Complex climbing-ripple cross-bedding in the upper olistoliths, attributed to intertidal environment. (D) Detail of C. showing the thinly laminated wackestone (light grey on the photograph).

stratigraphy with the autochthonous platform stratigraphy may help to identify the stratigraphic interval of the Doushantuo Formation, which is represented by the olistolith. This would therefore establish a maximum age for the mass wasting. The best exposed and almost continuous platform stratigraphic section for such a comparison is the Zhancumping section in Hubei province, located on the south-central Yangtze platform approximately 200 km north of the reconstructed platform margin location (Fig. 11).

Lithologies and depositional conditions at Zhancumping can possibly be correlated regionally with those in slide sheet No. 3 (Fig. 11). Thickness (several metres to tens of metres) and systematic variations in
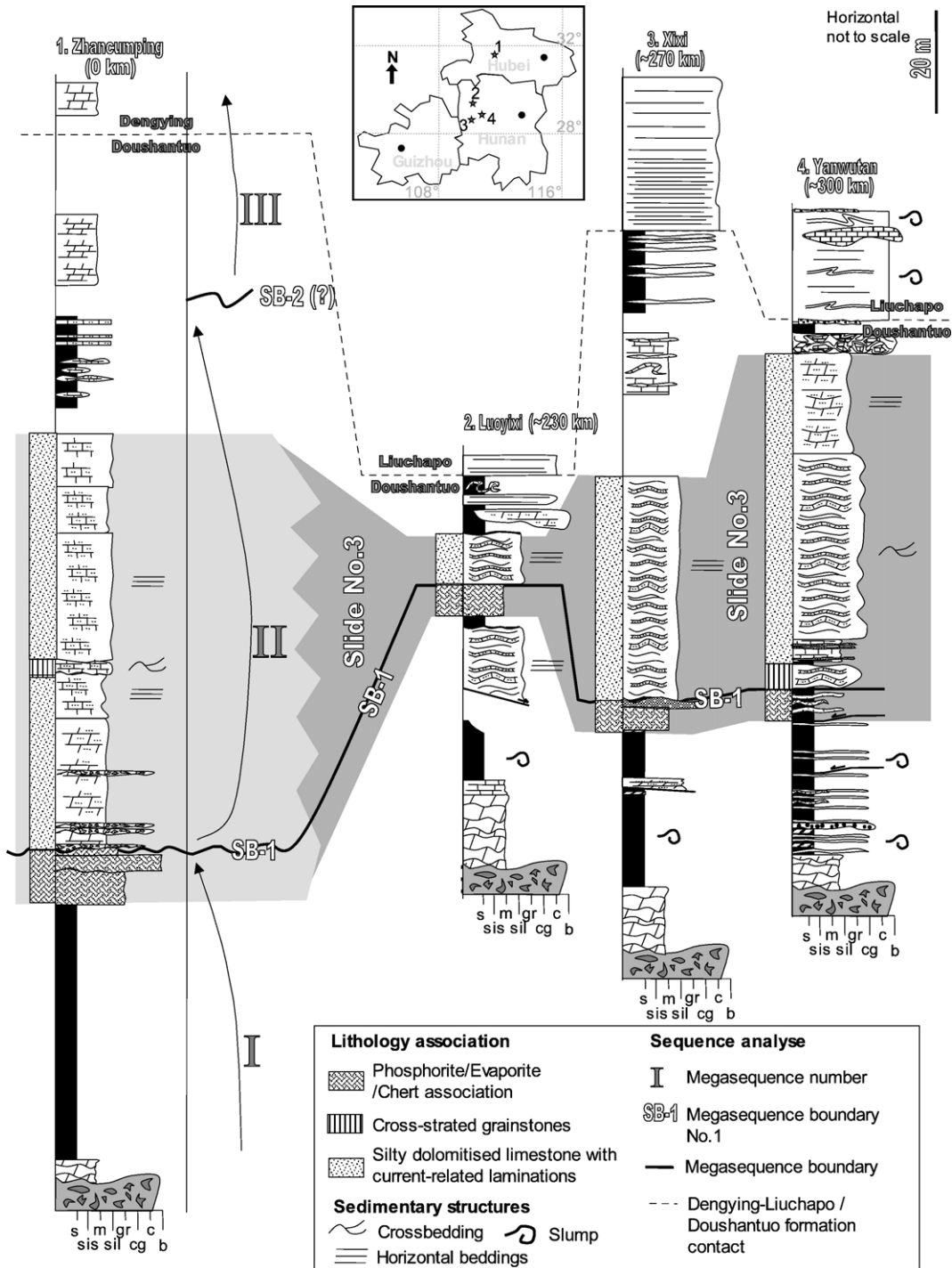
Fig. 11. Comparison between Zhancumping section, Hubei province, and the internal stratigraphy of slide sheet No. 3 (compiled from Luoyixi, Xixi and Yanwutan sections, Hunan province). Second-order megasequence analysis supports correlation of the partial sedimentary record in the allochthonous sections with the autochthonous record in Zhancumping section. The olistolith section may correspond to the top of megasequence 1 and the nearly all of megasequence 2. s: shale; sis: silty shale; m: mudstone; sil: silty limestone; gr: grainstone; cg: conglomerate; c: chert; b: breccia.

interpreted depositional environments in the Doush-antuo Formation argue for second-order megase-quences, which record relative sea level variations due to major tectonic movements rather than short-term climatic changes. Sedimentary packages are separated by erosive surfaces in Zhancumping section and by major facies shifts in Hunan slope sections, interpreted as megasequence boundaries. Allochthonous slide block no. 3 in Luoyixi, Xixi and Yanwutan sections shows facies shifts between the micrite-dominated facies association and the overlying grainstones with current-related laminations. This facies change marks the transition from a restricted shallow-water basin to a medium-energy shallow-water subtidal platform. Thus, the top of the phosphoritic interval represents a sequence boundary. The similitude in the sedimentary record of Zhancumping section and the slope sections

indicates that most olistoliths contain the top of parasequence I and a major part of parasequence II. Sliding at the platform margin may have occurred during the regressive period of parasequence II. In contrast to olistoliths of Hunan province, lithostrati-graphic correlation in the sections studied in Guizhou province is not possible.

5.2. Implications of evaporite presence

Primary evaporites may precipitate in shallow-water, enclosed continental lakes in hot climates, in saline ponds on Antarctic ice, in deep-water protected basins, or in coastal sabkhas (Cojan and Renard, 1997). The distinction between primary and secondary evaporites is problematic (Blatt, 1992). In the studied sections within the allochthonous slide blocks, the presence of shallow-
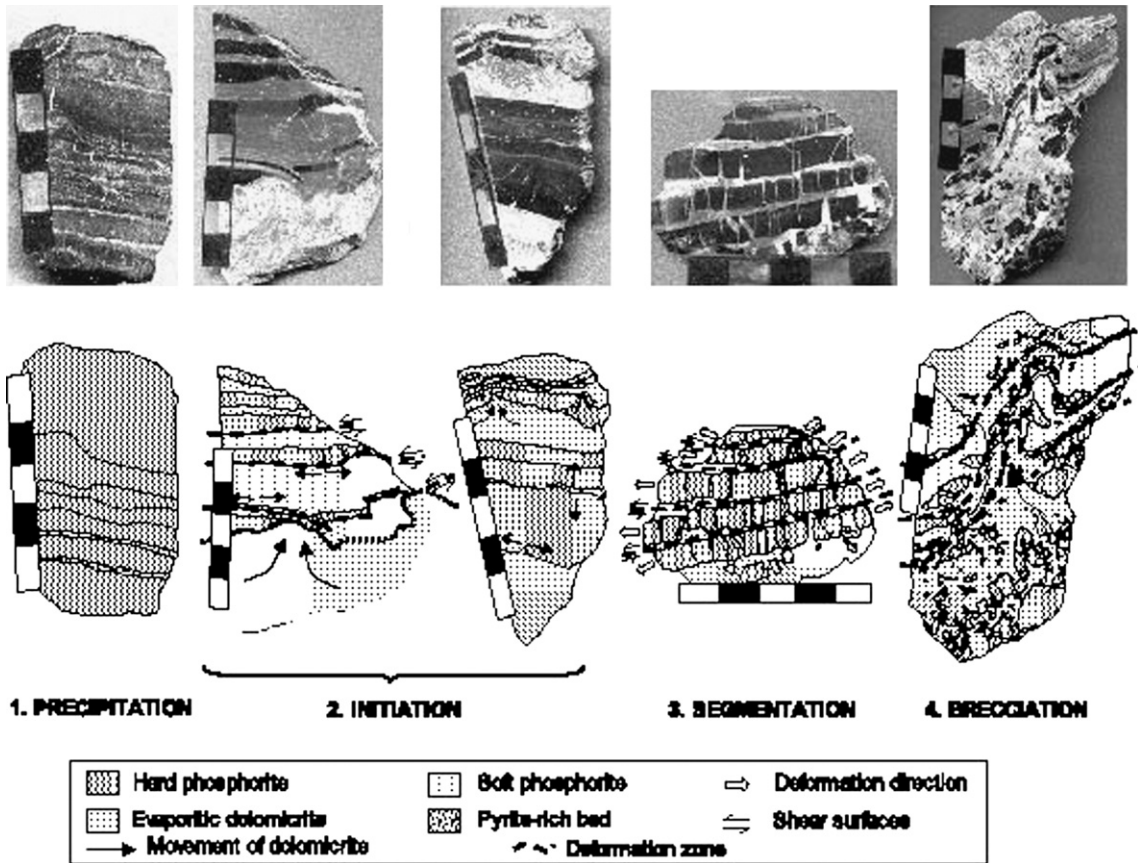

Fig. 12. Stages of evaporite-mediated breccia formation from hand sample (Xixi section, Hunan Province). 1. Initial phosmicrite, formed by concentration of dissolved fluoroapatite in the pore water and precipitation in the uppermost ten cm of unconsolidated sediment under hypoxic conditions due to protective biomats. 2. Ductile deformation. Dolomicrite deforms plastically due to evaporite dissolution. "Hard phosmicrite" hardground, in contrast, accommodates deformation by the creation of small fractures perpendicular to the bedding. Fig. 6B and C show deformation of (bio?) laminations by brittle segmentation of the black, "hard phosphorite" beds. 3. Brittle segmentation. Evaporitic dolomicrite matrix fills fractures and amplifies the fragmentation of "hard" phosmicrite, isolating cm-sized clasts. 4. Deformation. Evaporite diagenesis, dewatering, and sediment compaction produce rotated clasts and folds.
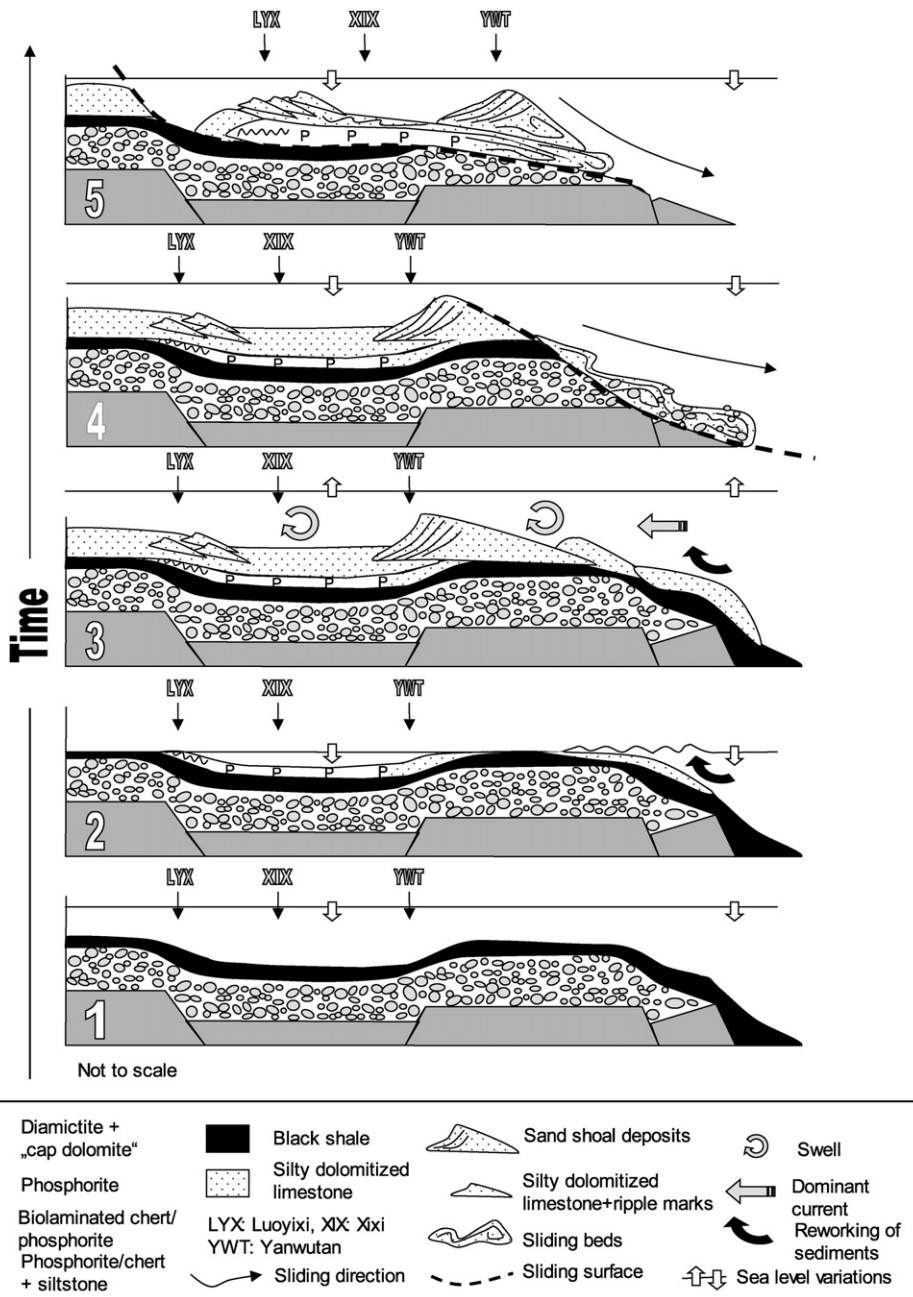
Fig. 13. Possible mechanism and sequence of slide initiation at the south-facing platform margin in Hunan and eastern Guizhou province. 1. Latest rift stage and beginning of thermal subsidence. Marinoan diamictites, "cap dolomite" and Doushantuo black shales fill a tectonically controlled bathymetry. 2. Phosmicrites are deposited during sea level low stand in (a) shallow-marine, enclosed intra-shelf basin(s) subjected to occasional storms. 3. Barriers become ineffective with sea level rise, and shelf-edge currents rework sediments and deposit coarse-grained carbonates. Lithologies and sedimentary structures in the slide blocks argue for shallow-water environments near the shelf edge, largely near the fair-weather wave base. 4 and 5. Initiation of olistostromes and slide sheets. The YWT, LYX, and XIX labels indicate the position of slide sheet no. 3 on the reconstructed platform margin before its sliding.

water facies (Facies 3) overlying an evaporite-bearing dolomite/phosphorite facies association (Facies 1 and 2) allows the interpretation of deposition in a shallow-marine, restricted basin. The lack of preferential crystal orientation argues in favour of the primary character of the evaporites (Tabakh et al., 1999), at least in Xixi

section. The irregular biomat surfaces may have supported the nucleation of evaporite crystals (Kendall and Plint, 1992). Apparently, shallow, enclosed basins evolved under a semi-arid climate with episodic evaporation, allowing water to become oversaturated with respect to sulfates. Hand sample inspection suggests four steps in the formation of the phosphorite breccias in Xixi section. We interpret the brecciation to be due to the ductile flow of evaporite-bearing dolomite, under low stresses, deforming overlying sediments (Fig. 12) during precipitation or dissolution of evaporites.

5.3. Paleoenvironmental evolution of the platform edge

Fault-controlled blocks inherited from the rifting phase (Wang and Li, 2003) or peritidal sand banks may have contributed to (partially or completely) isolate several platform margin mini-basins. In them, evaporites and phosphorites found a variety of depositional environments as a function of water depth, storm activity, seasonal variations in temperature and precipitation, and salinity. With sea level rise, barriers became ineffective. Platform currents reworked existing sediments and deposited grainstones. Our proposed evolution of the platform margin (Fig. 13) is consistent with the evolution of more proximal platform environments in Hubei and northern Hunan provinces (Vernhet, 2005).

Several mechanisms such as high pore-water pressure, formation of gas hydrates, and sea level fall may have caused the initiation of olistostromes and slide sheets. Sliding may have been facilitated by the well-stratified sediments resulting from the absence of bioturbation.

6. Conclusions

Depositional environments along the southern margin of the Yangtze platform, reconstructed in part from large slide blocks on the south-facing submarine slope, show the following features:

1. The platform margin in Hunan and eastern Guizhou provinces, represented in part by allochthonous slide sheets and olistostromes, shows unusual facies, ranging from a shallow marine, restricted-basin with episodic evaporitic conditions to medium-energy, wave-dominated, subtidal platform.
2. The internal stratigraphy of the allochthonous slide sheets may be correlatable with the autochthonous platform stratigraphy. Major mass wasting (slide sheet no. 3) may have occurred during a regressive period.

3. The parasequences recorded in stratigraphic column of the Zhancumping platform section may be correlatable at the basin scale, and may represent second-order variation of eustacy due to major tectonic events.

Acknowledgements

References

Babcock, L.E., Zhang, W., 2001. Stratigraphy, paleontology, and depositional setting of the Chengjiang lagerstätte (lower Cambrian), Yunnan, China. In: Peng, S.-C., Babcock, L.E., Zhu, M.-Y. (Eds.), Cambrian System of South China. Palaeoworld, vol. 13, pp. 66–86.

Babcock, L.E., Zhang, W., Leslie, S.A., 2001. The Chengjiang Biota: record of the early Cambrian diversification of life and clues to exceptional preservation of fossils. GSA Today 11 (2), 4–9.

Bahlburg, H., 2004. A review of the Snowball Earth hypothesis in light of recent scientific progress, Sino-German symposium: "Environmental and biological processes of the Cambrian explosion", Nanjing (China), pp. 12–13.

Baturin, G.N., 1982. Phosphorites on the Sea Floor. Elsevier, Amsterdam.

Blatt, H., 1992. Sedimentary Petrology. W.H. Freeman and Co., New York.

Chen, J.-Y., Bergstrom, J., Lindstrom, M., Hou, X.-G., 1991. Fossilized soft-body fauna. Research and Exploration 7 (1), 8–19.

Chen, J.-Y., Huang, D.-Y., Li, C.-W., 1999. An early Cambrian craniate-like chordate. Nature 402, 518–522.

Chen, D.-F., Dong, W.Q., Zhu, B.-Q., Chen, X.-P., 2004. Pb-Pb ages of Neoproterozoic Doushantuo phosphorites in South China: constraints on early metazoan evolution and glaciation events. Precambrian Research 132 (1-2), 123–132.

Cojan, I., Renard, M., 1997. Sédimentologie. Dunod, Paris.

Condie, K.C., 2003. Supercontinents, superplumes and continental growth: the Neoproterozoic record. In: Windley, Y.M., Dasgupta, S., Yoshida, M. (Eds.), Proterozoic East Gondwana: supercontinent assembly and breakup. Geological Society Publication House, London, pp. 1–21.

Condon, D., Zhu, M.-Y., Bowring, S., Yang, A., Jin, Y.-G., 2005. U-Pb ages from the Neoproterozoic Doushantuo Formation, China. Science 308 (5718), 95–98.

Corsetti, F.A., Hagadorn, J.W., 2000. Precambrian–Cambrian transition: Death Valley, US. Geology 28-4, 299–302.

Dobrzinski, N., Bahlburg, H., 2007. Sedimentology and environmental significance of the Cryogenian successions of the Yangtze platform, South China block. Palaeogeography, Palaeoclimatology, Palaeoecology 254, 100–119 (this volume), doi:10.1016/j.palaeo.2007.03.043.

Dobrzinski, N., Bahlburg, H., Strauss, H., Zhang, Q.-R., 2004. Geochemical climate proxies applied to the Neoproterozoic glacial succession on the Yangtze Platform, South China. In: Jenkins, G. (Ed.), The Extreme Proterozoic: Geology, Geochemistry and Climate. American Geophysical Union Monograph Series, vol. 146 (20 pp.).

Erdtmann, B.D., Steiner, M., 2001. Special observations concerning the Sinian–Cambrian transition and its stratigraphic implications on the central and SW Yangtze platform, China. In: Peng, S.-C., Babcock, L.E., Zhu, M.-Y. (Eds.), Cambrian System of South China. Palaeoworld, vol. 13, pp. 52–65.

Evans, D.A.D., Li, Z.X., Kirschvink, J.L., Wingate, M.T.D., 2000. A high-quality mid-Neoproterozoic paleomagnetic pole from South China, with implications for ice ages and the breakup configuration of Rodinia. Precambrian Research 100 (1-3), 313–334.

Eyles, N., Januszczak, N., 2004. "Zipper-rift": a tectonic model for Neoproterozoic glaciations during the breakup of Rodinia after 750 Ma. Earth Science Review 65 (1-2), 1–73.

Föllmi, K.B., Garrison, R.E., Grimm, K.A., 1991. Stratification in phosphatic sediments: illustrations from the Neogene of California. In: Einsele, Ricken W., Seilacher, A. (Eds.), Cycles and Events in Stratigraphy. Springer-Verlag, Berlin, pp. 492–507.

Frimmel, H.E., Folling, P.G., Eriksson, P.G., 2002. Neoproterozoic tectonic and climatic evolution recorded in the Gariep belt, Namibia and South Africa. Basin Research 14 (1), 55–67.

Germs, G.J.B., 1995. Neoproterozoic of southwestern Africa, with emphasis on platform stratigraphy and paleontology. Precambrian Research 73, 137–151.

Guo, Q.-J., Strauss, H., Liu, C.-Q., Goldberg, T., Zhu, M.-Y., Vernhet, E., Pi, D.-H., 2007. Carbon isotopic evolution of the terminal Neoproterozoic and Early Cambrian: evidence from the Yangtze Platform, South China. Palaeogeography, Palaeoclimatology, Palaeoecology 254, 137–154 (this volume), doi:10.1016/j.palaeo.2007.03.014.

Hoffman, P.F., Schrag, D.P., 2000. Snowball Earth. Scientific American 282, 68–76.

Hoffman, P.F., Schrag, D.P., 2002. The Snowball Earth hypothesis: testing the limits of global change. Terra Nova 14 (3), 129–155.

Hoffman, P.F., Kaufman, A.J., Halverson, G.P., Schrag, D.P., 1998. A Neoproterozoic Snowball Earth. Science 281, 1342–1346.

Hou, X.-G., Bergstrom, J., 2003. The Chengjiang fauna—the oldest preserved animal community. Paleontological Research 7 (1), 55–70.

Hou, X.-G., Bergstrom, J., Xu, G.-H., 2004. The lower Cambrian crustacean Pectocaris from the Chengjiang biota, Yunnan, China. Journal of Paleontology 78 (4), 700–708.

Hyde, W.T., Crowley, T.J., Baum, S.K., Peltier, W.R., 2000. Neoproterozoic "Snowball Earth" simulation with coupled climate/ice-sheet model. Nature 405, 425–429.

Jiang, G.-Q., Sohl, L.E., Christie-Blick, N., 2003. Neoproterozoic stratigraphic comparison of the Lesser Himalaya (India) and Yangtze block (south China): paleogeographic implications. Geology 31 (10), 917–920.

Kendall, A.C., Plint, A.G., 1992. Evaporites. In: Walker, R.G., James, N.P. (Eds.), Facies Models. Response to Sea Level Change, Geol. Ass. Canada Public. St. John's, Newfoundland, pp. 375–409.

Kenneth, J.H., Chen, H.-H., 1999. Geologic Atlas of China. Elsevier, Amsterdam.

Knoll, A.H., Xiao, S.-H., 1999. On the age of the Doushantuo Formation. Acta Micropaleontologica Sinica 16, 225–236.

Knoll, A., Fairchild, I.J., Swett, K., 1993. Calcified microbes in Neoproterozoic carbonates: implications for our understanding of the Proterozoic/Cambrian transition. Palaios 8, 512–525.

Li, Z.-X., Zhang, L., McA-Powell, C., 1995. South China in Rodinia: part of the missing link between Australia—East Antarctica and Laurentia? Geology 23-5, 407–410.

Liang, T.Y., Chang, A.C., 1984. On the characteristics and genesis of late Precambrian phosphorites associated with Gondwana plate. Geological Survey of India, Special Publication 17, 42–62.

Macouin, M., Besse, J., Ader, M., Gilder, S., Yang, Z., Sun, Z., Agrinier, P., 2004. Combined paleomagnetic and isotopic data from the Doushantuo carbonates, South China: implications for the, "Snowball Earth" hypothesis. Earth and Planetary Science Letters 224, 387–398.

Nogueira, A.C.R., Riccomini, C., Nóbrega Sial, A., Veloso Moura, C.A., Fairchild, T.R., 2003. Soft-sediment deformation at the base of the Neoproterozoic Puga cap carbonate (SW Amazon craton, Brazil): confirmation of rapid icehouse to greenhouse transition in snowball Earth. Geology 31-7, 613–616.

Pisarevsky, S.A., Wingate, M.T.D., McA. Powell, C., Johnson, S., Evans, D.D., 2003. Models of Rodinia assembly and fragmentation. In: Windley, Y.M., Dasgupta, S., Yoshida, M. (Eds.), Proterozoic East Gondwana: Supercontinent Assembly and Breakup. Geological Society Pub House, London, pp. 35–55.

Powell, C.M., Pisarevsky, S.A., 2002. Late Neoproterozoic assembly of East Gondwana. Geology 30-1, 3–6.

Runnegar, B., 2000. Loophole for Snowball Earth. Nature 405, 403–404.

Schwennicke, T., Siegmund, H., Jehl, C., 2000. Marine phosphogenesis in shallow-water environments: Cambrian, Tertiary, and recent examples. In: Glenn, C.R., Prevost-Lucas, L., Lucas, J. (Eds.), Marine Authigenesis: From Global to Microbial. SEPM, pp. 481–498.

Shu, D.-G., Morris, S.-C., Han, J., Zhang, Z.-F., Liu, J.-N., 2004. Ancestral echinoderms from the Chengjiang deposits of China. Nature 430, 422–428.

Steiner, M., 2001. Die fazielle Entwicklung und Fosiilverbreitung auf der Yangtze Plattform (Südchina) im Neoproterozoikum/frühesten Kambrium. Freiberger Forschungshefte 492, 1–26 (in German).

Sumner, D.Y., 2002. Decimetre-thick encrustations of calcite and aragonite on the sea-floor and implications for Neoarchean and Neoproterozoic ocean chemistry. Special Publication IAS 33, 107–120.

Tabakh, M.E., Grey, K., Pirajno, P., Schreiber, B.C., 1999. Pseudomorphs after evaporitic minerals interbedded with 2.2 Ga stromatolites of the Yerrida basin, Western Australia: origin and significance. Geology 27 (10), 871–874.

Trappe, J., 1998. Phanerozoic phosphorite depositional systems. A Dynamic Model for a Sedimentary Resource System, Lecture Notes in Earth Science, vol. 76. Springer-Verlag, Berlin.

Trappe, J., 2001. A nomenclature system for granular phosphate rocks according to depositional texture. Sedimentary Geology 145, 135–150.

Vernhet, E., 2005, Sedimentary processes, evolution, and paleoenvironmental reconstruction of the southern margin of the Ediacaran Yangtze platform (Doushantuo Formation, central China), PhD thesis, Freie Universität Berlin, 172 p.

Vernhet, E., 2007. Paleobathymetric influence on the development of the late Ediacaran Yangtze Platform (Hubei, Hunan, and Guizhou Provinces, China). Sedimentary Geology 197, 29–46.

Vernhet, E., Heubeck, C., Zhu, M.-Y., Zhang, J.-M., 2006. Large-scale slope instability at the southern margin of the Ediacaran Yangtze platform (Hunan province, Central China). Precambrian Research 148, 32–44.

Wang, J., Li, Z.-X., 2003. History of Neoproterozoic rift basins in South China: implications for Rodinia break-up. Precambrian Research 122, 141–158.

Xiao, S., Yuan, X., Steiner, M., Knoll, A.H., 2002. Macroscopic carbonaceous compressions in a terminal Proterozoic shale: a

systematic reassessment of the Miaohe Biota, South China. Journal of Paleontology 76 (2), 347–376.

Yin, C., Gao, L., Xing, Y., 2001. New observations on phosphatized spheroidal fossils in Sinian Doushantuoan phosphorites in Weng'an, Guizhou province. Acta Geologica Sinica 75 (2), 1–149.

Yin, C., Bengtson, S., Yue, Z., 2004. Silicified and phosphatized Tianzhushania, spheroidal microfossils of possible animal origin from the Neoproterozoic of South China. Acta Palaeontologica Polonica 49 (1), 1–12.

Yiqing, L., 1984. The Proterozoic–Cambrian phosphorite of China. Geological Survey of India, Special Publication 17, 207–210.

Zhu, M.-Y., Zhang, J.-M., Steiner, M., Yang, A.-H., Li, G.-X., Erdtmann, B.D., 2004. Sinian-Cambrian stratigraphic framework for shallow- to deep-water environments of the Yangtze platform: integrated approach. Progress in Natural Science 75–84 (Special Issue Aug.).